

FACULDADE DE ENGENHARIA DA UNIVERSIDADE DO PORTO

Relative acoustic localization with USBL (Ultra Short BaseLine)

Paula Alexandra Agra Graça

WORKING VERSION



Master in Electrical and Computers Engineering

Supervisor: José Carlos Alves

Co-supervisor: Bruno Ferreira

June 26, 2020

Resumo

Dispositivos robóticos programáveis como *Autonomous Underwater Vehicles* (AUVs) são excelentes meios para exploração subaquática, já que são capazes de executar missões de longa duração com variadas possibilidades de aplicação e objetivos. Neste sentido, o conceito de mola AUV surgiu como mecanismo útil que periodicamente recolhe dados dos AUVs em missão. Para que tal seja possível, é necessário implementar um sistema de localização e posicionamento robusto que permite aos AUVs encontrarem outros veículos de forma a aproximarem-se deles eficientemente.

A presente dissertação foca-se na implementação de um sistema que estima a posição relativa entre AUVs através do método *Ultra-Short Baseline* (USBL). Esta técnica baseia-se na determinação da diferença de fases entre sinais recebidos por um vetor de hidrofones.

Após a implementação e validação do sistema referido, este foi integrado num mecanismo existente que adquire e processa dados de quatro hidrofones. Na fase final, serão executados testes de campo e experiências num ambiente enclausurado, como o tanque do DEEC, seguido de um teste em ambiente real, em mar aberto.

Abstract

Robotic programmable devices such as Autonomous Underwater Vehicles (AUVs) are great means for underwater exploration, as they are capable of executing long term missions with many possible applications and goals. In this regard, the concept of mule AUVs arises as a valuable mechanism to periodically collect data from survey AUVs during the missions. In order to achieve this, a robust localization and positioning system needs to be implemented allowing the mule AUV to find the other vehicle and draw near it efficiently.

The present dissertation focuses on the implementation of a system which estimates the relative position between AUVs through the Ultra-Short Baseline (USBL) method. The technique relies on accurate estimation of the phase difference between signals received in a hydrophone array.

After implementation and validation of the mentioned system, it will be integrated in an existing mechanism which was specifically designed to acquire and process data from four hydrophones. In the final stage, field tests and experiments will be executed in a closed environment such as DEEC's tank, followed by a real environment test in open sea.

Contents

1	Introduction	1
1.1	Context and Motivation	1
1.2	Objectives	2
1.3	Document Structure	2
2	State of the Art	3
2.1	Underwater acoustic channel	3
2.1.1	Speed of sound	4
2.1.2	Multipath	4
2.1.3	Doppler Effect	5
2.1.4	Attenuation and signal-to-noise ratio	6
2.2	Range estimation for underwater localization	6
2.2.1	Received Signal Strength Indicator	6
2.2.2	Time Delay Estimation	7
2.3	Localization estimation	9
2.3.1	Triangulation	9
2.3.2	Trilateration	10
2.3.3	Multilateration	11
2.4	Positioning Systems	12
2.4.1	Long Baseline (LBL)	12
2.4.2	Short Baseline (SBL)	13
2.4.3	Ultra Short Baseline (USBL)	13
2.4.4	Inverted Systems	15
2.5	Commercial Solutions	15
2.6	Angle of arrival determinantion	16
2.7	Methods for optimizing sensor configurations	16
2.7.1	Crámer-Rao lower bound	16
3	Research Problem	19
3.1	Problem Statement	19
3.2	Hypothesis and Research Questions	20
3.3	Validation Methods	21
4	Proposed System	23
4.1	HDL Module Design	23
4.1.1	Hilbert Filter	23
4.1.2	Cordic	24
4.1.3	phasediff	24

4.1.4	phasemean	24
4.2	Angle of Arrival Calculation	24
5	Dynamic reconfigurable configuration method	25
5.1	Methodological approach	25
5.2	Systematic analysis of geometric configurations performance	25
5.2.1	Analytic Approach	25
5.2.2	Simulation Results	28
6	Conclusions	29
6.1	Summary	29
6.2	Main Contributions	29
6.3	Future Work	29
	References	31

List of Figures

2.1	Generic sound speed profile	4
2.2	Multipath	5
2.3	Three-Object Triangulation	10
2.4	Geometric Triangulation algorithm	10
2.5	Generic configuration of: a) LBL; b) SBL; c) USBL	12
2.6	USBL system configuration	14
3.1	Communication System	19

List of Tables

2.1	Overview of commercial solutions	16
5.1	Hydrophone geometric positions	27

Abbreviations

AUV	Autonomous Underwater Vehicle
BPSK	Binary Phase Shift Keying
CC	Cross-Correlation
DEEC	Departamento de Engenharia Electrotécnica e de Computadores
FIM	Fisher Information Matrix
FPGA	Field-Programmable Gate Array
FSK	Frequency-Shift Keying
GCC	Generalized Cross-Correlation
HDL	Hardware Description Language
LBL	Long Baseline
LOS	Line-of-sight
MF	Medium Frequency
ML	Maximum Likelihood
RMS	Root Mean Square
RSSI	Received Signal Strength Indicator
SBL	Short Baseline
SNR	Signal-Noise Ratio
TDE	Time Delay Estimation
TDOA	Time Difference of Arrival
TOA	Time of Arrival
TOF	Time of Flight
USBL	Ultra-Short Baseline

Chapter 1

Introduction

1.1 Context and Motivation

Today, the deep blue ocean still represents a relevant topic of research in the scientific community as it constantly rises new unexplained mysteries. Up to now, only 15% of the entire ocean floor is mapped based on collected data [17]. As such, it seems essential to create efficient research tools to improve the discovery of information.

Robotic autonomous underwater vehicles (AUVs) are great means for diverse applications in underwater exploration using variable resource requirements and duration, such as monitoring structures installed in shallow waters or exploring the deep ocean floor for scientific purposes. Particularly in long-term missions, the AUV is usually deployed using a docking system and it navigates underwater until the end of the mission, when it returns to the base station. Thus far, the data that is being collected is typically not accessible by any processing system or researchers.

A method that is used to resolve this limitation is employing additional mule AUVs, whose goal is to travel near the survey AUV, collect its data during the mission's term and return in a relatively short time period. This allows the data to be periodically processed during the mission, which facilitates the definition of future courses for the mission, such as shortening its duration or sending additional commands. In the mentioned localization system, high accuracy is key, as it avoids high energy consumption, saves up time in the inherently slow global process and avoids missing the AUV's underwater localization.

The described process can only be achieved if the mule AUV is able to locate the other AUV and draw near it. For that reason, a USBL (Ultra Short Base-Line) system will be implemented using an array of four hydrophones as acoustic receiver. This makes it possible to explore the difference among times of arrival of an acoustic signal to many hydrophones, allowing the calculation of the angle of arrival of the acoustic signal and thus the direction that the mule AUV should navigate. Additionally, using a synchronized transmission from the AUV being located, the mule AUV can also determine the distance to the acoustic source located in the survey AUV and thus its relative position to the mule AUV.

This dissertation intends to continue the work developed previously [4], in which a platform was created to acquire and process data from four hydrophones. The system to be implemented is carefully explained in the present document.

This research work falls under the scope of activities developed by the Center of Robotics and Autonomous Systems of INESC TEC. It is integrated in the GROW project which focuses on exploring the use of AUVs as data mules for long duration missions.

1.2 Objectives

The work aims to implement a system capable of determining the angle of arrival of known encoded acoustic signal and study processes to correct errors resulting from the deformation of propagation direction of the acoustic waves. In order to achieve that, it is proposed the implementation and validation of a digital signal processing system for FPGA technology, which determines the difference between the times of arrival of an encoded acoustic signal to four hydrophones. Thereafter, a software script will be able to take the system's output in order to estimate the intended angle of arrival. The system is then analyzed and methods are studied in order to improve the estimation process. Finally, the implemented system is validated experimentally with field tests.

1.3 Document Structure

The present document is partitioned into x chapters, which are summarized in this section.

Chapter 2

State of the Art

This chapter presents the fundamental concepts of underwater acoustics engineering for localization and positioning of aquatic autonomous vehicles.

2.1 Underwater acoustic channel

Although satellite based navigation systems are the most commonly used for positioning and localization at the air, the used radio signals are highly absorbed by the water and thus inappropriate for underwater localization and also for communications. Therefore, the state of the art solutions for long range localization and communications rely on the propagation of acoustic signals.

The natural limitations of acoustic channels combined with the properties of an underwater environment, result in challenges and limitations in developing communication and localization systems [23]:

- Long propagation delays;
- Variable speed of the acoustic signals;
- Reference nodes may have different drifting rates from each other due to water currents, which leads to uncertainties on the definition of absolute times and synchronization;
- Limited bandwidth
- Signals are bended due to sound speed variation along the water column and shadowed in many different surfaces, which may lead to the incorrect detection of the line-of-sight (LOS) signal;
- Attenuation and asymmetric signal-to-noise ratio, which arises from SNR depending on depth and frequency with complex behaviors that depend on the characteristics of the environment;

2.1.1 Speed of sound

The oceanic environment has a complex sound propagation model, as it comprises many variants in order to realistically represent underwater acoustics.

Acoustic signals' propagation speed is mainly related with two factors: compressibility and density. The water density can be characterized by the temperature, salinity and pressure, which is associated with depth. Figure 2.1 exhibits a generic sound speed profile in relation to depth. The water surface is commonly a mixed layer which results in an approximately constant sound speed. After this layer, it suffers a significative decrease, usually reaching the lower tangible speed, which results from the variation of temperature that characterizes the thermocline layer. From that point forward, pressure is the greatest influencer on the speed of sound, so it increases relatively proportionally to depth.

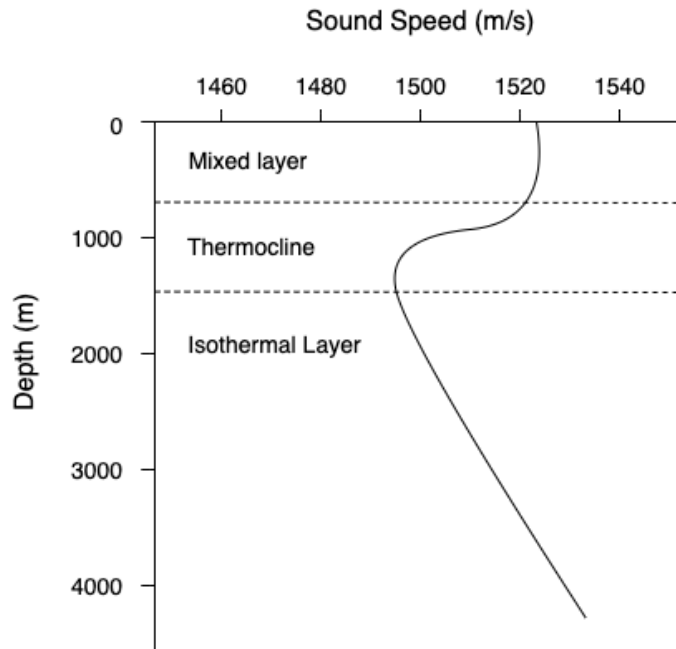


Figure 2.1: Generic sound speed profile

The empirical equation 2.1 [15] is a simplified translation of the behavior of the sound speed c in meters per second, with relation to the temperature T in $^{\circ}\text{C}$, the salinity S in parts per thousand and the depth z in meters.

$$c = 1449.2 + 4.6T - 0.055T^2 + 0.00029T^3 + (1.34 - 0.01T)(S - 35) + 0.016z \quad (2.1)$$

2.1.2 Multipath

Multipath occurs when a transmitting signal suffers reflection or refraction in a surface (e.g. water surface, ocean floor, dock's wall), leading to a change in its original characteristics. This phenomenon can affect the propagation speed, the energy and the total distance that the signal was predicted to travel. These altered signals in conjunction with constant movement of the receiver

makes it more complicated to accurately estimate the distance between the transmitter and the receiver, as well as determine the line-of-sight signal.

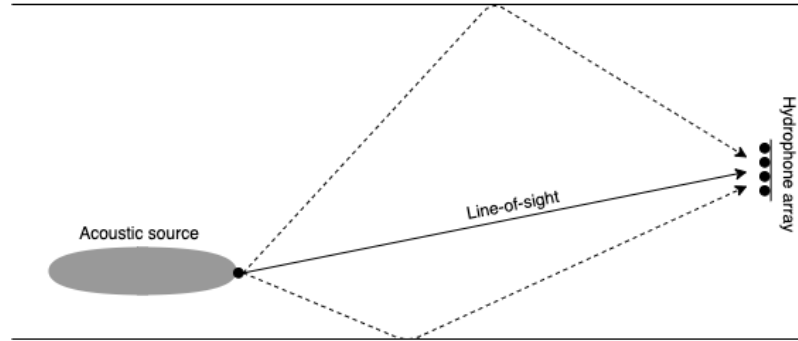


Figure 2.2: Multipath

In consequence, the underwater acoustic channel is qualified as a non-minimum phase system because it produces time-variant output responses.

2.1.3 Doppler Effect

In a communication and localization system between two entities moving with non-zero relative velocity, if a transmitter sends a signal with a certain operation frequency to the receiver, then the perceived frequency by the receiver will suffer a shift from the original signal. This frequency difference is expressed as a Doppler shift and explained by the Doppler Effect.

The magnitude of the generated frequency shift can be expressed as a ratio 2.2, where the transmitter-receiver velocity is compared to c , the speed of sound [21].

$$a = \frac{v}{c} \quad (2.2)$$

Autonomous Underwater Vehicles (AUVs) usually move with velocities in the order of few meters per second. Therefore, the a factor mentioned above has a significant value and needs to be considered when implementing synchronization systems, as well as developing estimation algorithms.

In certain localization and communication systems, it is critical to correct the Doppler effect because data can be compromised (e.g. FSK modulated signals, in which information is codified into frequency changes). A simple Doppler compensation process was proposed in [1], in a system to detect phase-modulated binary sequences using cross-correlation.

This phenomenon can also be explored to determine the relative velocity between two devices, by measuring the frequency deviation with respect to the frequency expected to be received.

2.1.4 Attenuation and signal-to-noise ratio

When considering underwater communication systems, it is essential to quantify the attenuation of the channel, i.e. the part of the signal's energy which is absorbed by the involving surrounding. In underwater channels, this absorbance is frequency variable and it is also dependent on physical characteristics of the water, as salinity and temperature.

The underwater acoustic channel has a particular model that describes its attenuation path loss $A(d, f)$, given in logarithmic scale by equation 2.3 [5].

$$10 \log(A(d, f)) = 10 k \log(d) + d 10 \log(a(f)) \quad (2.3)$$

From the equation, d is the distance from the transmitter to the receiver in kilometers (Km), f is the operating frequency in kilohertz (KHz), $10k\log(d)$ represents the spreading loss which describes how the sound level (in decibel, dB) decreases as the sound wave spreads, $d10\log(a(f))$ is the absorption loss that a signal suffers during its propagation path, k is the spreading factor which is related with the considered configuration (e.g. cylindrical, spheric, etc.), $a(f)$ is the absorption coefficient that can be obtained through the equation in [5].

Noise is another factor that is considered when analyzing a real underwater acoustic channel, as it defines the signal-to-noise ratio (SNR) that characterizes the channel. The SNR is dependent on the attenuation level which increases with frequency, and the noise which decays with frequency. Consequently, the SNR varies over the signal bandwidth and it is asymmetric. The equation 2.4 [21] expresses this relationship, where $S_d(f)$ represents the power spectral density of the transmitted signal.

$$SNR(d, f) = \frac{S_d(f)}{(A(d, f)) N(f)} \quad (2.4)$$

2.2 Range estimation for underwater localization

Underwater localization takes into consideration the distance between the target object to track and the reference point. As consequence, it is always relevant to apply methods which easily and effectively determine this range.

There are two main types of techniques that are used to achieve such objective: the Received Signal Strength Indicator (RSSI) and the Time Delay Estimation (TDE).

2.2.1 Received Signal Strength Indicator

The Received Signal Strength Indicator (RSSI) method is based on the strength of the signal that reaches the target. It determines the distance between the target and the reference node by analyzing the received signal strength and comparing it with an underwater attenuation model which is range dependent [15].

Since the underwater acoustic channel suffers from multipath, time variance and high overall path loss, the RSSI technique is not adequate for underwater applications.

2.2.2 Time Delay Estimation

Time Delay Estimation (TDE) mechanisms use a pair of nodes, the target and the reference point, to measure the range between them. This distance is based on the time that it takes for a signal to travel from the reference point to the target.

There are three main categories that divide TDE methods, which are Time Difference of Arrival (TDOA), Time of Arrival (TOA) and Time of Flight (TOF).

2.2.2.1 Time of Arrival

Time of Arrival (TOA) is interpreted as the time delay between the transmission of a signal in the reference node until its reception on the target node. Although this is the conceptually simplest method to employ, it requires synchronization between the nodes since the target entity needs to know the instance when the signal was sent to be able to calculate the difference.

Considering a generic transmitted signal $s(t)$, the received signal can be expressed as 2.5, where τ represents the time of arrival and $n(t)$ is white noise with zero mean [10].

$$r(t) = s(t - \tau) + n(t) \quad (2.5)$$

2.2.2.2 Time Difference of Arrival

The Time Difference of Arrival (TDOA) is a technique that compares the time of arrival of a signal to different hydrophones in order to estimate the angle of arrival of the acoustic signal. The array of reception hydrophones have known determined positions among them so that it is possible to compare the different times of arrival or phase differences. This method can be employed using a uni-directional signal or a round trip communication.

There are several algorithms and mathematical models that can be employed to execute the TDOA method, such as the Cross-Correlation and Maximum Likelihood.

2.2.2.3 Generalized Cross-Correlation

The Generalized Cross-Correlation (GCC) method is used to generically represent the relationship strength between two signals.

Considering two distanced hydrophones in the same environment and an acoustic source $s(t)$, $x1(t)$ and $x2(t)$ are the signals received by each of the two hydrophones. The equations 2.6 and 2.7 [2] express the mentioned signals in relation to $w1(t)$ and $w2(t)$ which are Gaussian noise coefficients uncorrelated with the source, τ that represent the delay and α which is an attenuation

function.

$$x1(t) = s(t) + w1(t) \quad (2.6)$$

$$x2(t) = \alpha s(t - \tau) + w2(t) \quad (2.7)$$

$$(2.8)$$

From these expressions, the generalized cross-correlation function between signals $x1(t)$ and $x2(t)$ is given by 2.9. The $G_{x1x2}(f)$ is the spectrum of the cross-correlation. The $\psi(f)$ represents a prefilter and it is essentially the distinctive parameter that originate various different methods of cross-correlation, since it should depend on different environments and properties as SNR.

$$R_{x1x2}(\tau) = \int_{-\infty}^{\infty} \psi(f) G_{x1x2}(f) e^{i2\pi f \tau} df \quad (2.9)$$

$$T = \tau_{max}[R_{x1x2}(\tau)] \quad (2.10)$$

Finally, the maximum value of $R_{x1x2}(\tau)$, expressed in 2.10, is the so called correlation peak and provides information about the time delay τ which is the main matter of Time Delay Estimation.

2.2.2.4 Cross-Correlation

After approaching the generalized method of cross-correlation, it is possible to better understand the Cross-Correlation (CC) method. There are two main variations of CC [2], which are the slow cross-correlation in the time domain and the fast cross-correlation in the frequency domain. The second approach is based on the Fast Fourier Transform as it locates the peak by analyzing frequency similarities between the signals.

Th Cross-Correlation technique uses a prefilter $\psi(f)$ equal to 1, as it is the simplest method of its kind.

2.2.2.5 Maximum Likelihood

The Maximum Likelihood (ML) method is a variation of Cross-Correlation which uses the prefilter $\psi(f)$ represented mathematically by 2.11, where $\gamma_{12}(f)$ is a function of spectrum of cross-correlation $G_{x1x2}(f)$ and spectrum of auto-correlations $G_{x1x1}(f)$, $G_{x2x2}(f)$ as expressed in 2.12 [2].

$$\psi(f) = \frac{|\gamma_{12}(f)|^2}{|G_{x1x2}(f)|[1-|\gamma_{12}(f)|^2]} \quad (2.11)$$

$$|\gamma_{12}(f)|^2 = \frac{|G_{x1x2}(f)|^2}{G_{x1x1}(f) \cdot G_{x2x2}(f)} \quad (2.12)$$

There is also a version of ML that uses the power spectral densities of the signals, which can be helpful for calculations in various applications.

2.2.2.6 Time of Flight

Time of Flight (TOA) measures essentially the round-trip time communication between two nodes. The target node sends a signal to the reference node, which has an integrated transponder that responds transmitting a signal back to the target. The TOA is then estimated as the time interval from the moment the first signal is transmitted until the moment the second signal is received by the same node.

This method may be used without additional synchronization systems as it assumes that the response signal is sent immediately after the received one and the intrinsic transmitting delays are known.

The accuracy of this technique depends mainly on the environment conditions, which include the water properties and the surrounding reflection surfaces which cause multipath. Therefore, the mechanism is susceptible of variable errors according to the location and characteristics of its employment.

2.3 Localization estimation

In networks with multiple nodes is typical to use localization estimation to establish position relationships between elements. The operation principal is usually to have a set of reference nodes with known positions so that it is possible to determine the relative positions between each reference node and the target.

An extensive comparison of different localization schemes for underwater sensors networks can be consulted in [6].

2.3.1 Triangulation

Triangulation is a method of localization based on the measurement of angles which are related to the reference beacons and the target object.

2.3.1.1 Three-Object Triangulation

The simplest method of this category is the Three-Object Triangulation, which considers a configuration as illustrated in figure 2.3. It is assumed that the location of the beacons is pre-configured and the environment is obstacle-free. λ_{12} is the angle formed by the intersection of the straight lines [O,1] and [O,2]. Similarly, λ_{31} is the angle formed by the intersection of the straight lines [O,1] and [O,3]. Using these two sets of nodes, we can trace circumferences that include their coordinates and as a consequence their intersection will correspond to the location of the target.

Although this is a very straightforward technique to implement, it does not cover all possible scenarios, namely when the three beacons and the object are all placed in the same circumference or when the environment has obstacles between nodes.

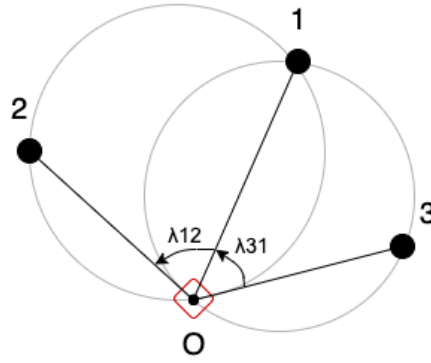


Figure 2.3: Three-Object Triangulation

2.3.1.2 Geometric Triangulation algorithm

A more complex method relies on the Geometric Triangulation algorithm.

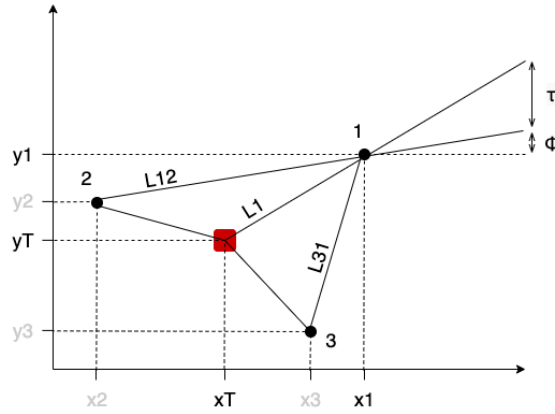


Figure 2.4: Geometric Triangulation algorithm

Considering a Cartesian plane with defined lengths $L1$, $L12$ and $L31$, as shown in image 2.4, it is possible to establish trigonometrical relationships that estimate the location of the object within the created triangular areas. The position of the target is given by coordinates (xT, yT) and can be calculated through equations 2.13 and 2.14. $(x1, y1)$ represents the location of beacon 1 and $L1$ is the distance between this beacon and the object. The trigonometric relationships for calculating the mentioned variables can be consulted in [8].

$$xT = x1 - L1 * \cos(\phi + \tau) \quad (2.13)$$

$$yT = y1 - L1 * \sin(\phi + \tau) \quad (2.14)$$

2.3.2 Trilateration

Trilateration is a technique that does not rely on calculations using angles but instead it uses distances to locate an object.

Considering a scenario with three reference beacons, the distance between the target and each one of the beacons is taken as the radius of a circumference. By doing this, it is possible to obtain three circumferences that intersect each other. With only two circumferences, there are two possible locations for the object, however, when added the third circumference the exact location is obtained. The 2D coordinates are obtained by solving systems of equations with the circle equation 2.15 [19], where (x_i, y_i) is the beacon coordinates and r_i is the distance between the beacon and the object.

$$(x - x_i)^2 + (y - y_i)^2 = r_i^2 \quad (2.15)$$

Trilateration is commonly used in underwater acoustic localization, as it used to find a relative position of the target in two dimensions and additionally determines the depth as third dimension, by using a pressure sensor with high accuracy.

2.3.3 Multilateration

Multilateration is a generalization of the trilateration technique, as it uses the same conceptual principal with multiple reference beacons instead of exactly three. In this method, the employment of $n+1$ nodes will allow to determine n coordinates [7]. For example, determining the position (x, y, z) of a target, would require to resolve a system of equations using 2.16. (x_i, y_i, z_i) is the coordinates of the beacon and d_i is the distance between the beacon and the target.

$$(x - x_i)^2 + (y - y_i)^2 + (z - z_i)^2 = d_i^2 \quad (2.16)$$

Distributed mechanisms, such as multilateration, are usually divided in three phases of positioning [6]:

- Distance estimation between the reference nodes and target object, usually using TDOA or TOF mechanisms;
- Position estimation, usually obtained by solving a system of linear equations through mathematical efficient techniques;
- Final refinement of the measurement in order to improve accuracy.

As an alternative to solve localization issues using circumferences, multilateration can also take advantage of a hyperbola-based localization method. Considering a target at (x, y) and three reference beacon with coordinates (x_i, y_i) , (x_j, y_j) and (x_k, y_k) , we have that the difference between times of arrival t_i and t_j to nodes i and j , respectively, can be related to the distance between nodes, as expressed in 2.17 [7]. d_i and d_j are the distance from node i and j , respectively, to the target object.

$$d_i - d_j = c * (t_i - t_j) = \sqrt{(x - x_i)^2 + y - y_i)^2} - \sqrt{(x - x_k)^2 + y - y_k)^2} \quad (2.17)$$

2.4 Positioning Systems

Positioning systems are used to track the underwater position of a vehicle or other object, in relation to reference structures of transponders called *baseline stations*. These systems are classified based on the distance between the baseline stations. The configurations that will be explained are Long Baseline (LBL), Short Baseline (SBL), Ultra Short Baseline (USBL) and the inverted versions of all above.

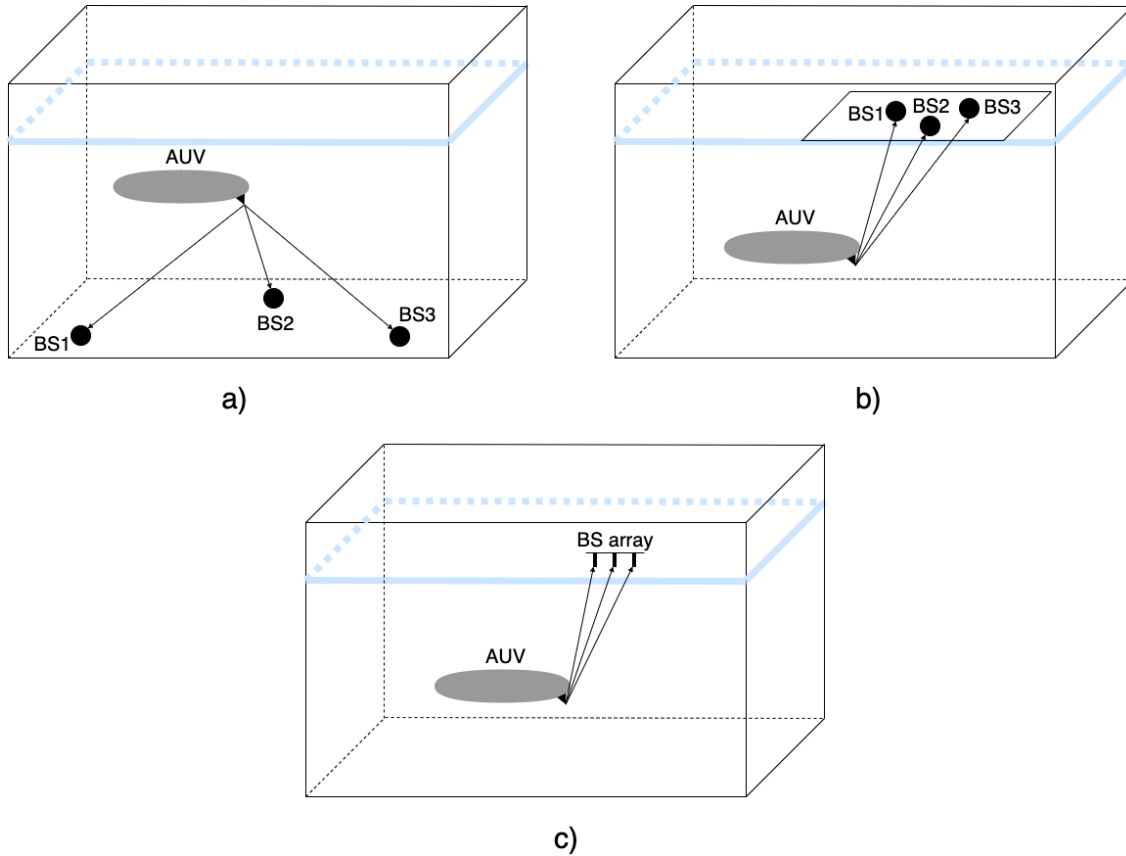


Figure 2.5: Generic configuration of: a) LBL; b) SBL; c) USBL

2.4.1 Long Baseline (LBL)

Long Baseline systems use a positioning method with large distances between baseline stations, with range typically from 50m to more than 2000m and usually similar to the distance between object and transponders [2]. A typical LBL configuration is represented in figure a) 2.5.

The LBL method uses at least three transponder stations deployed usually on the sea floor, allowing to execute trilateration. Additionally, a transducer is integrated on the object to be tracked.

A complete localization procedure starts with the vehicle sending an acoustic signal which is received by the transponders. Thereafter the transponders transmit a response and, by analyzing the Time of Flight of the communication, the system can determine the distance between the vehicle and each base station. Then the relative position of the vehicle is determined through trilateration. Additionally, if the transponders have known geographic positions, it is possible to infer the vehicle geographic position.

As this technique presents large distances between the object and the base stations, the typical 1m to few centimeters accuracy is considered to be high because it will not compromise the localization of the vehicle.

2.4.2 Short Baseline (SBL)

Short Baseline systems are characterized by having distances around 20m to 50m between baseline stations [23] and use an operation procedure similar to the LBL method. However, the transponders are usually placed in a moving platform, which assures a fixed relative position between them. A typical SBL configuration is represented in figure b) 2.5.

The position of the vehicle to be tracked can be determined by translating the Time of Flight between the multiple transponders and the object into a distance value, which is achieved by equation 2.18 [24]. The t_i corresponds to the propagation time of the signal from the vehicle to the i th transponder, c is the speed of sound, $[x_{b_i}, y_{b_i} \text{ and } z_{b_i}]$ is the coordinate position of the transponder.

$$\sqrt{(x_{b_i} - x)^2 + (y_{b_i} - y)^2 + (z_{b_i} - z)^2} = c * t_i \quad (2.18)$$

In a SBL system, when the distance between baseline stations is increased the accuracy improves and, contrarily, when the mentioned distance decreases the accuracy deteriorates, which can raise some deployment challenges.

2.4.3 Ultra Short Baseline (USBL)

Ultra short baseline systems are composed essentially by one baseline station, with an array consisting of several traducers distanced typically less than the wavelength [16], and a transponder integrated on the object to be tracked. It is usually used in underwater positioning in shallow areas of the sea, as represented in figure c) 2.5.

Similarly to the previously mentioned procedures, the USBL positioning method relies on the Time of Flight of the exchanged signals. However, the traducers are too spatially close from each

other to execute an accurate trilateration. Instead, it is measured the phase difference or time-delay difference of the received signal between every traducer, in order to estimate the azimuth and distance to the acoustic source.

Assuming a three dimensional scenario for the positioning system, as represented in figure 2.6, the object's coordinates are given by equations 2.20, 2.21 and 2.22 [22]. The λ corresponds to the wavelength of the of the transmitted signal which depends on its operation frequency, f , and it is affected by the speed of sound c , as represented equation 2.19. The d represents the distance between hydrophones, ψ_{12} and ψ_{22} are the phase difference between H2 and the other two hydrophones, H is the height of the target object, X is the distance of the target along the x-axis direction, Y is the distance of the target along the y-axis direction and l is the slant distance of the target to the hydrophone.

$$c = f * \lambda \quad (2.19)$$

$$l^2 = X^2 + Y^2 + H^2 \quad (2.20)$$

$$\psi_{12} = \frac{2\pi}{\lambda} [\sqrt{l^2} - \sqrt{(d-X)^2 + d^2 + H^2}] \quad (2.21)$$

$$\psi_{22} = \frac{2\pi}{\lambda} [\sqrt{l^2} - \sqrt{X^2 + (d-Y)^2 + H^2}] \quad (2.22)$$

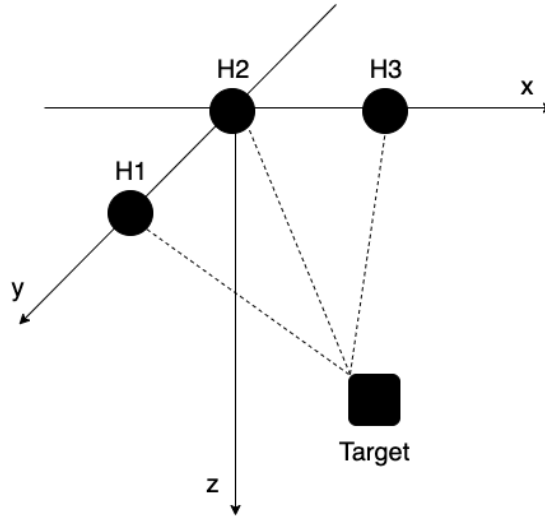


Figure 2.6: USBL system configuration

This is a broadly used technique due to its convenient set up, which allows to have predefined measurements in the order of tens of centimeters and does not require AUV navigation area for the deployment. However it presents the lowest accuracy, comparatively with LBL and SBL, since an error of few centimeters can be realistically corresponding to an inaccuracy of several meters in the position of the object to be tracked.

2.4.4 Inverted Systems

All the previously mentioned positioning techniques use a configuration in which the vehicle to be tracked has a single transducer and there is an external set of transponder to determine the positioning of the said object. However, there is the possibility to benefit from the inverse configuration in some applications. Therefore, there are also the iLBL, iSBL and iUSBL methods, which have the same operation principals as LBL, SBL and USBL, respectively.

2.5 Commercial Solutions

There are several commercial solutions for underwater positioning using the ultra-short baseline method. In this section, it will be presented some of the available devices in the market, indicating their main properties and capabilities. Table 2.1 summarizes the systems with most relevance to the present work. The Medium Frequency (MF) bandwidth is attributed to devices whose manufacturer did not specified the actual frequency range.

Evologics produces the S2C R USBL series of acoustic modems [14], with Sweep Spread Carrier (S2C) technology [13] which uses a broad frequency range to propagate over large distances with reduced noise. The devices have a fixed 0.01m slant range accuracy and a 0.1 degree bearing resolution. These are essentially divided into two groups:

- High speed mid-range devices: contains the 18/34 transceivers family [11], which presents various options for the USBL antenna beam pattern and it is optimal for transmission in horizontal channels.
- Depth rated long-range devices: includes the 12/24 transceiver [12], which have a directional (70 degrees) USBL antenna and it is optimal for transmission in vertical channels.

Sonardyne markets the Ranger 2 systems. The Micro-Ranger 2 [20] is very easy to use without previous experience and it is appropriate for shallow waters, achieving accuracy of 0.2%. The Mini-Ranger 2 is ideal for nearshore missions and it is used for simultaneous tracking of various mobile targets, whose position is updated every 3 seconds.

Applied Acoustics offers the Easytrak USBL Systems, which includes the processing software for estimating the position. The Alpha Portable 2655 consists in a very compact structure that includes an array transducer and is capable of reaching a 10cm slant range resolution and a 2 degree RMS.

Kongsberg produces the HiPAP family of transducers [18], which can use the Cymbal acoustic protocol (PSK) or the frequency shift (FSK) modulation technique. Particularly the HiPAP 352 is the model with higher number of active transducers and is able to reaches 0.02m of range accuracy.

Company	System	Bandwidth(kHz)	Connection(kbps)	Range(m)
Evologics	S2C R 18/34D USBL	18-34	up to 13.9	3500
	S2C R 12/24 USBL	12-24	up to 9.2	6000
Sonardyne	Micro-Ranger 2	MF	0.2-9	995
	Mini-Ranger 2	MF	0.2-9	995
Applied Acoustics	Easytrak Alpha Portable 2655	MF	n.d.	500
Kongsberg	HiPAP 352	21-31	n.d.	5000

Table 2.1: Overview of commercial solutions

2.6 Angle of arrival determination

2.7 Methods for optimizing sensor configurations

When evaluating the performance of a localization system which integrates a multiple sensor configuration, it is essential to resort to widely used methodologies to prove its validity and accuracy. This section is dedicated to explore some commonly employed methodologies.

2.7.1 Crámer-Rao lower bound

In this thesis, it is conducted a study based on the Crámer-Rao lower bound, which is generally used to generate a *so-called uncertainty ellipse* [3] that represents the spatial variance distribution of the estimated position. The overall desired result is to find the minimum variance value that is related to the chosen configuration geometry, which indicates that it is the optimal solution for estimating a certain position. This method utilizes the Fisher Information matrix (FIM), whose components translate characteristics of the observation vector.

In order to avoid loss of generality, it is considered a set of N sensors and a settled position for the target, the acoustic source, defined by $s_t = [x_{s_t}, y_{s_t}, z_{s_t}]^T$. In addition, the position of each sensor is defined as $r_i = [x_{r_i}, y_{r_i}, z_{r_i}]$ and, consequently, the measurement of distance between each sensor and the source is defined as $d_i = \|s_t - r_i\|$.

Thereafter, the observations vector will be formulated containing the observed times-of-arrival (TOA) of the signal from the acoustic source to each one of the hydrophones, considering their geometric position. These times contain a noise vector component, which can be approximated to to a Gaussian distribution $n_i \sim \mathcal{N}(\mu, \sigma^2)$. The samples can be calculated through the expression 2.7.1, where it is considered an initial time of arrival t_0 . Additionally, c represents the sound speed underwater.

$$t_i = t_0 + \frac{\|d_i\|}{c} + n_i$$

After having the observations matrix, it is established the condition to formulate the Fisher Information matrix, $I(d)$, which results into equation 2.7.1.

$$I(d) = \nabla_d t(d)^T \Sigma^{-1} \nabla_d t(d)$$

$\nabla_d t(d)$ is the gradient matrix of the observations vector regarding d_i , whereas Σ is the covariance matrix, in which the diagonal contains the standard deviation of the components of each noise vector, construed as $(\sigma_1^2, \sigma_2^2, \dots, \sigma_N^2)$.

Thereby, all conditions are established to proceed to the actual calculation of the Fisher Information matrix. After formulated, it will indicate the quantity of information that a certain sensor configuration can give about a position in space. Hence the goal is to obtain the maximum achievable information. By calculating the determinant of FIM it is possible to deduce the minimum *uncertainty ellipsoid* and therefore the configuration's best possible performance. Therefore, the optimal solution is given by the maximum output of the determinant of FIM.

Additionally, it is possible to detail this information by calculating the actual size of the axis that compose the *uncertainty ellipsoid*. This is achieved by calculating the square mean root of the eigenvalues of $I(d)$, which correspond to each axis size.

Further explanation about the methods used in a deeper exploration of the Crámer-Rao lower bound can be consulted in [3], which serves as guide to investigate other scenarios of application of this theorem. However, the mentioned concepts were all the necessary for the approach on this dissertation.

This same process is adopted in this dissertation. All steps specifically taken for this study are declared in section 5.2 of the present document.

Chapter 3

Research Problem

This chapter intends to clarify the problem addressed by the present dissertation.

3.1 Problem Statement

As previously mentioned in chapter 1, it is considered a scenario where an AUV is taking part on a long-term underwater mission. When it is in course, the moving survey AUV periodically sends known signals to the surface with a pinger, so it can be identified. The mule AUV, which is provided with a three dimensional array of hydrophones, receives the signal and estimates the position of the other AUV to navigate near it. The described communication system is illustrated in figure 3.1.

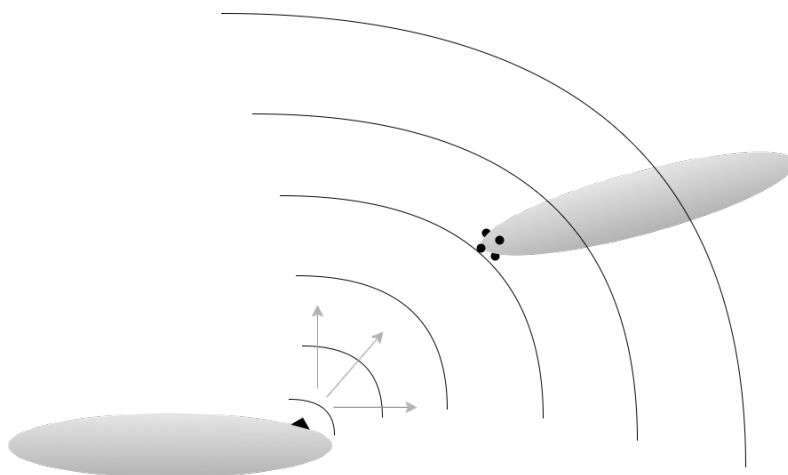


Figure 3.1: Communication System

This partial system was developed in previous dissertations and research work, which can be better understood in [4]. Briefly, the system consists on a transducer of four hydrophones forming a 3D array deployed on the mule AUV. This array will receive the same signal wave front. The system then calculates the cross-correlation between the received and expected signals, which is a BPSK modulated binary sequence. The cross-correlation peak indicates the distance

between AUVs and it is calculated with timing resolution corresponding to 1 sampling period of the acquired signal, which in the developed systems corresponds approximately to 6mm (with a sampling frequency of 244kHz).

Since we are referring to an USBL system and due to the limitations in dimension of the AUV that will integrate this system, the hydrophones have to be placed within a few centimeters from each other. For this reason, the obtained time resolution by using only the cross-correlation, corresponding to a maximum distance accuracy of approximately 6mm, will not be enough for the calculation of the angle of arrival of the sound wave. Thus, in this thesis it is intended to refine this measurement by additionally calculating the phase differences of the arriving signals to each hydrophone.

Upon having this measurement refined, the information of the phase difference between hydrophones, as well as additional data from modules already implemented, will serve as base to develop a software mechanism that estimates the angle of arrival of the received signal to the hydrophone array.

Finally, as an effort to improve the underwater localization system, a set of tests have to be performed in order to evaluate the robustness and estimation accuracy of the developed system. This study intends to prove the hypothesis declared in 3.2 and consequently respond to some of the defined research questions.

3.2 Hypothesis and Research Questions

This dissertation intends to complement previous research work by adding the design of an integral hardware model and respond to a core research hypothesis which serves as fundamental investigation purpose.

The first part of the developed work focuses on the practical implementation of a HDL model which has as premise the following idea: *"Implementing a system that utilizes the phase differences between the arriving signals to an array of hydrophones, increases the accuracy of the time of arrival determination of the current system, which consequently improves the angle of arrival estimation."*

The second part of the research work focuses on the study and experimentation with methods that improve the localization accuracy for underwater applications. This research hypothesis can be stated as:

"Using a real-time dynamic reconfigurable hydrophone array improves the underwater localization accuracy"

Attending the proposed hypothesis, the topics that are intended to be explored and discussed in this thesis's work can be summarized in the following research questions:

- **RQ1:** *How should a system be implemented so it is capable of calculating phase differences between arriving signals at four different hydrophones and, simultaneously, be compatible with the available space in the FPGA?*
- **RQ2:** *What method should be adopted in order to efficiently estimate the angle of arrival of a signal to an array of four hydrophones?*
- **RQ3:** *What metrics should be used to evaluate which hydrophone configuration is optimal for a certain angle of arrival?*
- **RQ4:** *How should the system be developed in order to improve the vision angle of the hydrophone array?*

These questions summarize the main topic points which are explored in the scope of this thesis and are the essential inquiries that it intends to answer.

3.3 Validation Methods

The validation of scientific work is a key factor to demonstrate how reliable and effective it is. In this thesis, three essential methods are used to validate the functionality of the developed techniques:

- **Simulation**

The considered immediate approach to evaluate the functionality and behavior of the system consists in creating a set of simulation procedures which are as close as possible to the real environment and the physical system. These simulations were made as MATLAB scripts carefully designed to integrate realistic parameters, such as expected environment noise and other limitations.

- **Scientifically recognized methods**

When composing a system, it can be useful comparing the studied approach with widely used methods which are recognized in the scientific community as robust and trustworthy. By doing this, we can gain a level of confidence in the developed system and in the obtained results.

- **Field experiments**

After having the analytical methods and simulations coherent, it is essential then to test the system in a real environment in order to understand if the system still works correctly when real conditions are added. By testing it in a real application it is possible to take conclusions about its robustness and consider improvements or refinements for the system.

Chapter 4

Proposed System

This chapter is dedicated to the presentation and overall explanation of the developed system, highlighting its capabilities, the used methodologies and overall design strategies. The system will be presented in two distinct sections. The first component is the HDL module, which falls into the spectrum of hardware design and requires insight on hardware development and good practices. The second section relies on software development to complement the functionality of the mentioned module, so that is possible to deliver the desired result.

4.1 HDL Module Design

The system which is proposed to be implemented in this research work has as input 4 signals which are received by hydrophone of the array, and outputs an average phase difference between all combinations of pairs of hydrophones.

- ver regras basicas de hardware development - sistema sincrono, available clock cycles globais - hardware limitations - tamanho das entradas

1. Hilbert Filter
2. CORDIC
3. phasediff
4. phasemean

4.1.1 Hilbert Filter

- matematica brevemente, equação base, resposta impulsional, ganho, coeficientes e ordem usada
- schematics
- explicar design decisions
- descrever brevemente flow do sinal no hardware

4.1.2 Cordic

- descrição do que faz, matematica (?)
- entradas e saídas, clocks, ROM

4.1.3 phasediff

- pequeno esquema
- 1 sub

4.1.4 phasemean

- pequeno esquema
- N accumulated

apresentar esquema global menos pormenorizado

4.2 Angle of Arrival Calculation

- explicar ambiguidade de fase do sinal
 - explicar calculos de angulo de chegada (script + matematica) com base nas posições dos hydrophones e do angulo de chegada
 - por simulação, conclui que para distancias muito longe (quantizar) não faz diferença ter o TOA e basta os TDOA

Chapter 5

Dynamic reconfigurable configuration method

5.1 Methodological approach

- tenho sistema que estima os MSE, erro de azimute e elevação, para certas configuração consegue-se perceber padroes nos erros (e.g. erro aumenta com afastamento da source -> ao longe variações pequenas de angulo podem indicar deslocação da estimação grande)
- de entre 8 hidrofonos, escolher sempre 3 (+1 no nariz) que minimizam o erro de estimação
- Configurações com vista direta: seccionar campo de visão para cada hidrofone
- aumenta o ângulo de visão para posições no espaço (literature review de valores tipicos)

5.2 Systematic analysis of geometric configurations performance

One of the aspects that can be studied to improve the localization estimation is analyzing the best sensor configuration that could be used for a certain scenario. Therefore, it was used the Crámer-Rao lower bound method to do a systematic study on the performance of several hydrophone configurations to be applied in many situations. The study serves as decision method for sensor configurations both applied in an AUV or in a situation without a vehicle.

The fundamental thought process and mathematical notation used in [2.7.1](#) are applied in the study that will be explained next.

5.2.1 Analytic Approach

Following the logical approach for the process, there are three essential steps that can be differentiated:

1. Formulate the observations vector
2. Calculate the Fisher Information Matrix (FIM)

3. Calculate the determinant of FIM and draw conclusions

In this thesis, the number of used hydrophones per estimation is four, so all calculations will be presented for this specific case.

Firstly, the observations vector is formulated based on an initial time of arrival t_0 , which is given by a synchrony mechanism integrated in the global communication system, and the time-of-arrival based on the vectors that connect the hydrophone positions, r_i , to the considered source, s_t . For a more realistic approach, it is also considered an added noise component that can be approximated to to a Gaussian distribution $n_i \sim \mathcal{N}(\mu, \sigma^2)$.

The four observations vector are then formulated as expressed in 5.5.

$$t_1 = t_0 + \frac{s_t - r_1}{c} + n_i \quad (5.1)$$

$$t_2 = t_0 + \frac{s_t - r_2}{c} + n_i \quad (5.2)$$

$$t_3 = t_0 + \frac{s_t - r_3}{c} + n_i \quad (5.3)$$

$$t_4 = t_0 + \frac{s_t - r_4}{c} + n_i \quad (5.4)$$

$$(5.5)$$

Then, addressing the second step, all conditions are set to calculate the FIM, $I(d) \in \mathbb{R}^{3 \times 3}$. In order to do so, if it is considered $d_i = \|s_t - r_i\|$ as the distance between each sensor and the source, the gradient of the observations vector can be expressed as shown in 5.6.

$$\nabla_{dt}(d) = \frac{1}{c} \begin{bmatrix} \frac{d_1^T}{\|d_1\|} \\ \frac{d_2^T}{\|d_2\|} \\ \vdots \\ \frac{d_N^T}{\|d_N\|} \end{bmatrix} \quad (5.6)$$

Additionally, the added noise component which is introduces to the calculations is present in the covariance matrix used in the FIM equation, which is represented as in 5.7.

$$\Sigma = \begin{bmatrix} \sigma_1^2 & 0 & 0 & 0 \\ 0 & \sigma_2^2 & 0 & 0 \\ 0 & 0 & \sigma_3^2 & 0 \\ 0 & 0 & 0 & \sigma_4^2 \end{bmatrix} \quad (5.7)$$

Overall, the conditions to obtain the FIM matrix are established and, after some mathematical formulation, it is expressed as 5.8. This expression can be validated by a similar study made on TOA based optimal positioning [9].

$$I(d) = \frac{1}{c^2} \left[\sum_{n=1}^N \frac{d_i d_i^T}{\|d_i\|^2} \frac{1}{\sigma_i^2} \right] \quad (5.8)$$

The final step is to calculate the determinant and find its relation to the volume of the *uncertainty ellipsoid*. As mentioned before, in 2.7.1, the determinant of the Fisher Information matrix gives a deterministic value that represents the quantity of information that we can obtain and, therefore, the objective is to maximize it, by respecting the condition $\text{argmax } \det(I(d))$, and consequently minimizing the volume of the ellipsoid.

5.2.1.1 Uncertainty Sphere

Firstly, it is necessary to choose a set of hydrophone configurations to be tested by the developed simulation environment. Therefore, considering the geometry of an AUV it was formulated a matrix containing nine hydrophones, from which are chosen four at a time to compose the configuration. Matrix 5.1 represents positions of the the nine hydrophones, where each column expresses the coordinates of each hydrophone, r_i , where the value of x_i is in the first row, the value of y_i in the second row and the value of z_i in the third row. Since the configuration has to be three dimensional, it is considered that the hydrophone r_1 , in the first column, always integrates the configuration since it is the only one in a different plan.

	r1	r2	r3	r4	r5	r6	r7	r8	r9
x	q	0	0	0	0	0	0	0	0
y	0	0	0	w	-w	e	e	-e	-e
z	0	w	-w	0	0	e	-e	e	-e

Table 5.1: Hydrophone geometric positions

In order to evaluate the obtained determinant values, a way to give physical meaning to this result is to analyze it through the uncertainty volume. However, in an initial approach the ellipsoid was not considered and instead an uncertainty sphere was analyzed. The radius of the uncertainty sphere, u_s , is expressed as 5.9, which translates the three ellipsoid axis into a single mean radius that originates a figure of the same volume.

$$u_{sphere}(d) = \sqrt[3]{\sqrt{\det(I(d)^{-1})}} \quad (5.9)$$

By doing this, we know are looking to find the $\text{argminur}(d)$ which indicates that the error that originates that uncertainty radius is minimal.

5.2.1.2 Uncertainty Ellipsoid

- eigenvalues give the length of each axis of ellipsoid

$$u_{\text{ellipsoid}}(d) = \sqrt[2]{\text{eig}(I(d)^{-1})} \quad (5.10)$$

5.2.2 Simulation Results

All the concepts and notions before mentioned were applied in a simulated series of scenarios, where it is attempted to take conclusions about optimal positioning of the sensors for performance improvement. As such, the conditions of the simulation as well as the results of the study are hereinafter explained.

As mentioned before, the key to evaluate the performance when adopting this method is to analyze the determinant of the inverted FIM or, alternatively, the matrix's eigenvalues.

... Layout some results ...

Ideias:

1—

- tabela que para cada posição de 4 hidrofones, indica:
- raio de incerteza maximo e posição no espaço onde ocorreu
- raio de incerteza minimo e posição no espaço onde ocorreu
- desvio padrao de todos os pontos no espaço
- uncertainty ellipsoid

2—

plot do raio de incerteza para todas as posições no espaço de uma certa configuração

5.2.2.1 Conclusions

Chapter 6

Conclusions

6.1 Summary

6.2 Main Contributions

6.3 Future Work

References

- [1] J. M. F. Magalhães. Improving time of arrival estimation using encoded acoustic signals. Master's thesis, Faculty of Engineering of the University of Porto, Porto, jul 2018.
- [2] B. M. R. Bharathi and A. R. Mohanty. Underwater sound source localization by emd-based maximum likelihood method. *Acoustics Australia*, 46(2):193–203, 2018.
- [3] A. N. Bishop, B. Fidan, B. D. O. Anderson, K. Doğançay, and P. N. Pathirana. Optimality analysis of sensor-target localization geometries. *Automatica*, 46(3):479–492, 2010.
- [4] A. M. Bonito. Acoustic system for ground truth underwater positioning in deec's test tank. Master's thesis, Faculty of Engineering of the University of Porto, Porto, jul 2019.
- [5] D. E. Chaitanya, C. V. Sridevi, and G. S. B. Rao. Path loss analysis of underwater communication systems. In *IEEE Technology Students' Symposium*, pages 65–70. 2011.
- [6] V. Chandrasekhar, W. KG Seah, Y. S. Choo, and H. V. Ee. Localization in underwater sensor networks: survey and challenges. In *WUWNet '06: Proceedings of the 1st ACM international workshop on Underwater networks*, pages 33–40, 2006.
- [7] M. Erol-Kantarci, H. T. Mouftah, and S. Oktug. A survey of architectures and localization techniques for underwater acoustic sensor networks. *IEEE Communications Surveys & Tutorials*, 13(3):487–502, 2011.
- [8] J.S. Esteves, A. Carvalho, and C. Couto. Generalized geometric triangulation algorithm for mobile robot absolute self-localization. In *2003 IEEE International Symposium on Industrial Electronics*, volume 1, pages 346–351, Rio de Janeiro, Brazil, 2003.
- [9] B. Ferreira, A. Matos, and N. Cruz. Optimal positioning of autonomous marine vehicles for underwater acoustic source localization using toa measurements. In *2013 IEEE International Underwater Technology Symposium (UT)*, pages 1–7. IEEE, 2013.
- [10] S. Gezici. A survey on wireless position estimation. *Wireless Personal Communications*, 44(3):263–282, 2008. Springer Science & Business Media.
- [11] EvoLogics GmbH. 18/34 communication and positioning devices, 2018. [Online]. Available: <https://evologics.de/acoustic-modem/18-34> [Accessed Jan. 26, 2020].
- [12] EvoLogics GmbH. S2c r 12/24 usbl communication and positioning device, 2018. [Online]. Available: <https://evologics.de/acoustic-modem/12-24/usbl-serie> [Accessed Jan. 26, 2020].
- [13] EvoLogics GmbH. S2c technology, 2018. [Online]. Available: <https://evologics.de/s2c-technology> [Accessed Jan. 26, 2020].

- [14] EvoLogics GmbH. Underwater usbl positioning systems, 2018. [Online] Available: <https://evologics.de/usbl>. [Accessed Jan. 26, 2020].
- [15] F. B. Jensen, W. A. Kuperman, M. B. Porter, and H. Schmidt. Fundamentals of ocean acoustics. In *Computational Ocean Acoustics*, pages 3–17. Springer Science & Business Media, second edition, 2011.
- [16] K. G. Kebkala and A. I. Mashoshinc. Auv acoustic positioning methods. *Gyroscopy and Navigation*, 8(1):80–89, sep 2017.
- [17] J. Liang. Fifteen percent of ocean floor now mapped, Jun 2019. [Online] Available: <https://www.deeperblue.com/fifteen-percent-of-ocean-floor-now-mapped/>. [Accessed Oct. 28, 2019].
- [18] Kongsberg Maritime. Hipap - high precision acoustic positioning, 2016. [Online]. Available: <https://www.kongsberg.com/maritime/products/Acoustics-Positioning-and-Communication/acoustic-positioning-systems/hipap-models/> [Accessed May 2, 2020].
- [19] A. P. Pandian, T. Senjyu, S. M. S. Islam, and H. Wang. Weighted trilateration and centroid combined indoor localization in wifi based sensor network. In *Proceeding of the International Conference on Computer Networks, Big Data and IoT (ICCB - 2018)*, pages 163–166, jul 2019.
- [20] Sonardyne. Micro-ranger 2 shallow water usbl system, 2020. [Online]. Available: <https://www.sonardyne.com/product/micro-ranger-2-shallow-water-usbl-system/> [Accessed Feb. 3, 2020].
- [21] M. Stojanovic and J. Preisig. Underwater acoustic communication channels: Propagation models and statistical characterization. *IEEE Communications Magazine*, 47(1):84–89, 2009.
- [22] D. Sun, J. Ding, C. Zheng, and W. Huang. An underwater acoustic positioning algorithm for compact arrays with arbitrary configuration. *IEEE Journal of Selected Topics in Signal Processing*, 13(1):120–130, mar 2019.
- [23] H. P. Tan, R. Diamant, W. K. G. Seah, and M. Waldmeyer. A survey of techniques and challenges in underwater localization. *Ocean Engineering*, 38(1):1663–1676, 2011.
- [24] X. You, Y. Wu, M. Zhu, X. Li, and L. Zhang. Low complexity short baseline localization algorithm based on taylor expansion. In *2019 IEEE International Conference on Signal Processing, Communications and Computing*, pages 1–5. IEEE, 2019.